

# **Superlattice formation of faceted PbS quantum dots with three-dimensionally aligned crystal orientation**

Kohki Mukai\*, Satoshi Fujimoto, and Fumimasa Suetsugu

*Graduate School of Engineering, Yokohama National University*

*79-5 Tokiwadai, Hodogaya-ku, Yokohama 240-8501, Japan*

\*E-mail: mukai-kohki-cv@ynu.ac.jp

We report the successful fabrication of a superlattice film composed of PbS colloidal quantum dots (QDs) with a three-dimensionally coincident crystal orientation. Faceted QDs with a truncated octahedral shape were prepared and deposited in a solvent on a pyramidal microhole array prepared on a Si (100) substrate. During the deposition, facets of neighboring QDs came into contact with each other in the aligned microholes. The three-dimensional crystal orientation alignment was confirmed by X-ray pole figure mapping. Such QD superlattice film with aligned crystal orientation can contribute to the realization of high-energy conversion efficiency of semiconductor solar cells.

In recent years, the quantum dot (QD) superlattice structure has attracted much attention in the context of achieving high energy conversion efficiency for semiconductor solar cells. Such structures can absorb light of a wide range of wavelengths with suppressed heat loss with the aid of intermediate bands<sup>1)</sup>. Fabrication of the superlattice structure has been attempted using Stranski–Krastanow-type QDs by the epitaxial growth method for the development of solar cells<sup>2)</sup>. However, it is difficult to grow a dislocation-free crystal with uniform QDs and the high energy conversion efficiency expected for such systems has not yet been realized. Chemical synthesis of colloidal QDs can be undertaken at low cost to achieve a uniform structure with high three-dimensional symmetry. It is also known that a closely-packed QD film (superlattice) is formed in a small area, as observed by electron microscopy, when colloidal QDs are deposited on a substrate in a solvent<sup>3-6)</sup>. In the film, the crystal orientation of each QD is independent of the others. If the colloidal QDs have the same crystal orientation in the superlattice, coupling of electron wave functions between QDs will be strengthened and carrier mobility will be improved<sup>7)</sup>. We have shown that the crystal orientation of QDs can be aligned in the closely-packed structure by depositing faceted QDs over several days<sup>8)</sup>. However, the packed structure obtained on a flat substrate was similar to a polycrystalline state in which closely-packed small areas were randomly gathered, and the alignment of the crystal orientation of QDs was only along the direction perpendicular to the substrate. We also showed that large-area QD superlattices, where QDs are arranged with long periodicity, can be fabricated by depositing QDs on a Si template on which pyramidal microholes were periodically arranged<sup>9-11)</sup>. In this letter, we report that a large-area QD superlattice film with coinciding crystal orientation in three dimensions can be fabricated by depositing faceted QDs on a pyramidal microhole array.

PbS QDs with a truncated octahedral structure were synthesized<sup>12, 13)</sup>. The faceted QDs self-assembled over a small area with facets of individual QDs facing each other, as shown in Fig. 1. The facets seen were eight (111) planes and six (100) planes. A 2-mm square template, in which pyramidal microholes with a side length of 3  $\mu\text{m}$  were periodically arranged, was prepared on a Si (100) substrate by electron beam lithography and anisotropic wet etching using a KOH solution. QDs dispersed in toluene were introduced dropwise onto the template. Then, the QDs were deposited in

toluene on a substrate and the superlattice film was formed on evaporation of the toluene. The evaporation speed was changed by exposing the sample to air or sealing it in a container under high toluene vapor pressure. Our previous experiments indicated that the self-assembling of QDs in solvent takes about 3 days. If the evaporation speed of solvent is faster, QDs are forcibly pushed downward by the liquid level and they gather relatively irregularly on the substrate. Therefore, in the experiments, the case where the solvent was evaporated in 20 minutes and the case where QDs were slowly deposited on a template over 7 days were compared. The QD film covered almost the entire template. Surface images of the film were observed by scanning electron microscopy (SEM).

Figure 2 shows SEM images obtained at the edge of the QD film, indicating how QDs filled the pyramidal microholes. In the case of rapid deposition, some voids were observed in the film in the microholes, suggesting that they were not densely filled, probably because there was not enough time for QDs to move on the template surface before they were set at the stable position for dense packing. In the case of slow deposition, the QDs were preferentially deposited in the microholes and the QD film was dense and void free owing to sufficient time being available for QDs to settle in their positions over 7 days.

The QD orientation in the superlattice film was evaluated by X-ray diffraction (XRD). The texture coefficient (TC), defined by the intensity of the observed diffraction peaks and their database intensity over  $\theta$ - $2\theta$  measurements, was used to determine which crystal plane of the QDs oriented preferentially in a direction parallel to the substrate surface<sup>14</sup>). The TC for the (hkl) crystal plane can be expressed as

$$TC(hkl) = \frac{I(hkl)/I_0(hkl)}{\frac{1}{n}\sum[I(hkl)/I_0(hkl)]} , \quad (1)$$

where  $I(hkl)$  is the measured intensity,  $I_0(hkl)$  is the database intensity, and  $n$  is the number of observed peaks. The sum is for all observed peaks. When a specific crystal plane is preferentially oriented along a direction, its peak intensity becomes stronger than others and the TC in the direction attains a high value. Using XRD pole figure measurements, in-plane distribution of the crystal orientation can be evaluated. In this study, the diffraction intensity was measured while rotating samples by an in-plane

angle of  $\varphi$  with a fixed  $2\theta$  Bragg angle of  $26^\circ$  for the PbS (111) plane. The measurement was repeated to complete the pole figure map while changing the elevation angle of  $\psi$ , which corresponds to the angle between the PbS (111) plane and the substrate surface in this case. In other words,  $\psi$  indicates which crystal planes are parallel to the substrate surface.

Figure 3 shows the results of TC measurements using a flat substrate and the template with varying deposition times. After XRD measurements, we chose four clear peaks corresponding to the crystal planes (111), (200), (220), and (311). Regardless of the shape of substrate and the deposition time, TC value suggesting the prior orientation of the (220) crystal plane was the largest. In addition, on increasing the deposition time from 20 minutes to 7 days, TC value for (220) plane became larger. Furthermore, when the deposition time was long, TC value for (200) plane became larger on the template, suggesting that a QD alignment that was not realized on a flat substrate had been generated in this case.

Figure 4 shows the pole figure maps when QDs were deposited for 7 days. Below the maps, the  $\varphi$  dependence of the X-ray diffraction intensity at  $\psi = 35^\circ$  and  $55^\circ$ , which correspond to the (220) and (200) planes, is shown (see Fig. 5). The diffraction intensities are represented by the cross sections of the concentric circles with red dashed lines in the pole figure map. On a flat substrate, the diffraction intensities of the (220) plane produced substantially uniform circles, indicating that the in-plane orientation distribution was isotropic. The (200) plane was hardly observed. On the other hand, on the template, since the intensity distribution of both planes was four-fold symmetric, the pyramidal hole affected the in-plane orientation of QDs. In detail, the intensities of the four (200) peaks were almost the same, whereas the intensities of the four (220) peaks could be represented by two alternately arranged pairs of peaks of equal intensity.

Based on the above findings, the arrangement of the QDs in the microholes can be discussed. The microholes formed by wet etching of single crystal Si showed a regular quadrangular pyramidal shape composed of (111) facets. It was expected that the microholes would be filled with QDs with a body-centered tetragonal (bct) alignment while QDs would self-assemble with a body-centered cubic alignment on a flat substrate<sup>8)</sup>. The bct structure is equivalent to a deformed body-centered cubic or face-centered cubic structure. The faceted QDs in the pyramidal microhole can be filled

with a bct alignment in two ways as shown in Fig. 5 with their (111) facets facing each other.

In the case of Fig. 5(a), where QDs were self-assembled so that the PbS (200) planes were parallel to the substrate surface, the QD arrangement in the pyramid hole was rotational symmetry of order 4. In this case, the angle between the (111) plane and the substrate surface is  $55^\circ$ , which is equivalent to  $\psi$ . When the diffraction intensity was measured while rotating in the in-plane direction ( $\phi$ ), the Bragg condition was satisfied for the (111) plane every time  $\phi$  rotated by 90 degrees, so that four peaks appeared, as shown in Fig. 4. The four broad peaks in Fig. 4 suggest that the arrangement of QDs was partially disturbed. Two possible disturbances are conceivable. One case involves incomplete faceting of QDs, while the other could be attributed to QDs rotating in a free direction on a flat area other than the pyramidal microholes on the template.

In the case shown in Fig. 5(b), where PbS (220) planes are parallel to the substrate surface, QDs in the pyramidal hole were arranged in a rotationally symmetric manner of order 2. In this case, the angle between the (111) plane and the substrate surface is  $35^\circ$ . During the measurement of the  $\phi$  dependence of the diffraction intensity, the Bragg condition for the (111) plane was satisfied every time  $\phi$  rotated by  $180^\circ$ , and two equally spaced peaks appeared with respect to  $\phi$ . However, since the same packing state rotated by  $90^\circ$  can exist in a template at the same time, there were actually four peaks. This model explains why the diffraction curve for the (220) plane was two pairs of two peaks, as shown in Fig. 4.

In summary, we have fabricated a superlattice film composed of PbS QDs whose plane orientation was aligned. QDs with an octahedron truncated shape were prepared and when they were deposited on a flat substrate, the (220) plane was aligned parallel to the substrate surface. When depositing QDs on a template of a pyramidal microhole array for 7 days, the preferential alignment of the (200) plane orientation became strong in addition to that of the (220) plane orientation. Pole figure measurements suggested that the crystal orientation of QDs on the template coincided three-dimensionally. These results were explained by a model in which faceted QDs were filled with a bct structure in the pyramidal holes with (111) planes touching each other and the direction of QD alignment was forcibly adjusted by the nanoholes. The technique presented here is applicable to the fabrication of high-efficiency solar cells using QD superlattice.

## **Acknowledgments**

This research was supported by the Canon Foundation, the Nohmura Foundation for Membrane Structure's Technology, and the Iwatani Naoji Memorial Foundation.

## References

- 1) T. Nozawa, Y. Arakawa, *Appl. Phys. Lett.* **98**, 171108 (2011).
- 2) T. Sogabe, Y. Shoji, M. Ohba, K. Yoshida, R. Tamaki, H.-F. Hong, C.-H. Wu, C.-T. Kuo, S. Tomic, and Y. Okada, *Sci. Rep.* **4**, 4792 (2014).
- 3) C. B. Murray, C. R. Kagan, and M. G. Bawendi, *Science* **270**, 1335 (1995).
- 4) L. Cademartiri, J. Bertolotti, R. Sapienza, D. S. Wiersma, G. Freymann, and A. Ozin, *J. Phys. Chem. B* **110**, 671 (2006).
- 5) R. Li, K. Bian, T. Hanrath, W. A. Bassett, and Z. Wang, *J. Am. Chem. Soc.* **136**, 12047 (2014).
- 6) W. V. D. Stam, A. P. Gantapara, Q. A. Akkerman, G. Soligna, J. D. Meeldijk, R. V. Roij, M. Dijkstra, and C. D. M. Donega, *Nano Lett.* **14**, 1032 (2014).
- 7) P. K. Santra, A. F. Palmstrom, C. J. Tassone, and S. F. Bent, *Chem. Mater.* **28**, 7072 (2016).
- 8) K. Mukai, S. Fujimoto, and F. Suetsugu, *Jpn. J. Appl. Phys.* **57**, 04FS02 (2018).
- 9) Y. Shimizu, I. Morimoto, S. Nakashima, and K. Mukai, *Abstr. 26th Int. Microprocesses and Nanotechnology Conf.*, 2013, 8P-11-57.
- 10) K. Mukai, *J. Nanosci. Nanotechnol.* **14**, 2148 (2014).
- 11) K. Mukai, A. Hirota, Y. Shimizu, and S. Nakashima, *Semicond. Sci. Technol.* **30**, 044006 (2015).
- 12) M. A. Hines, G. D. Scholes, *Adv. Mater.* **15**, 1844 (2003).
- 13) H. Choi, J.H. Ko, Y.-H. Kim, and S. Jeong, *J. Am. Chem. Soc.* **135**, 5278 (2013).
- 14) E. Güneri, F. Göde, S. Çevik, *Thin Solid Films* **589**, 578 (2015).

## Figure Captions

**Fig. 1.** Transmission electron microscopy image of QDs with facets. The synthesis temperature was 130 °C.

**Fig. 2.** SEM images of QD film deposited on the microhole array: (a) deposition time of 20 minutes, and (b) deposition time of 7 days. The film edge was observed so that the images of QDs and the pyramidal holes were obtained simultaneously.

**Fig. 3.** Texture coefficient (TC) of four XRD peaks. For the deposition time of 20 minutes and 7 days, a comparison was obtained for the case concerning a microhole array and that concerning a flat substrate.

**Fig. 4.** Pole figure maps when QDs were deposited over 7 days on the microhole array and the flat substrate. Below the maps, the  $\varphi$  dependence of the X-ray diffraction intensity is shown at  $\psi = 35^\circ$  and  $55^\circ$ , which correspond to the PbS (220) and PbS (200) planes, respectively.

**Fig. 5.** Scheme of faceted QDs packed in a microhole: (a) (200) plane of QDs is parallel to the substrate surface, and (b) (220) plane is parallel to the substrate surface. X-ray diffraction was obtained for the (111) plane of PbS QDs during pole figure measurement.

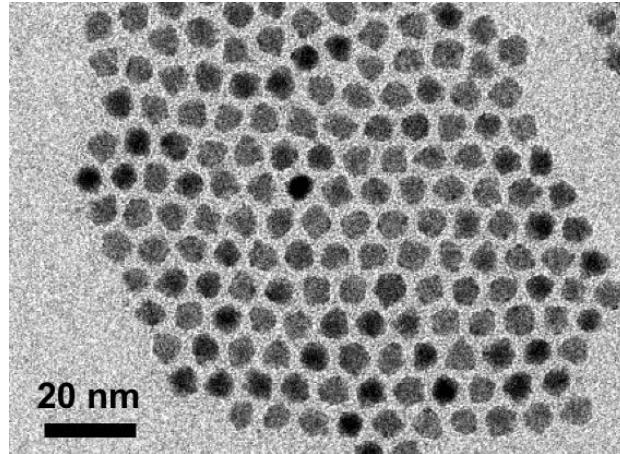
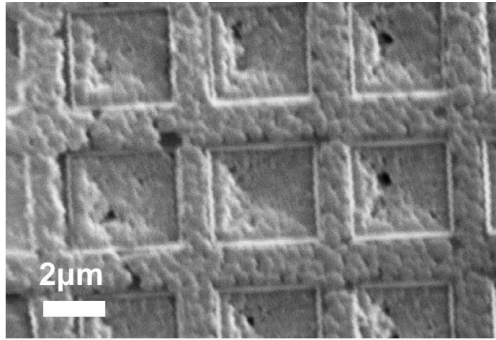
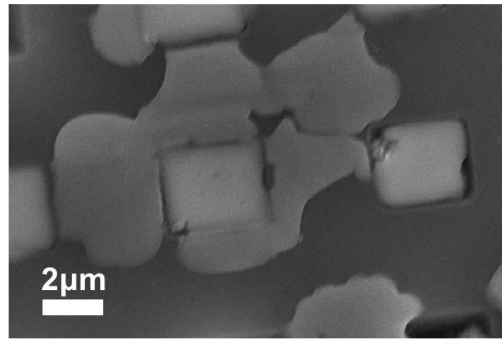


Fig. 1



(a)



(b)

Fig. 2

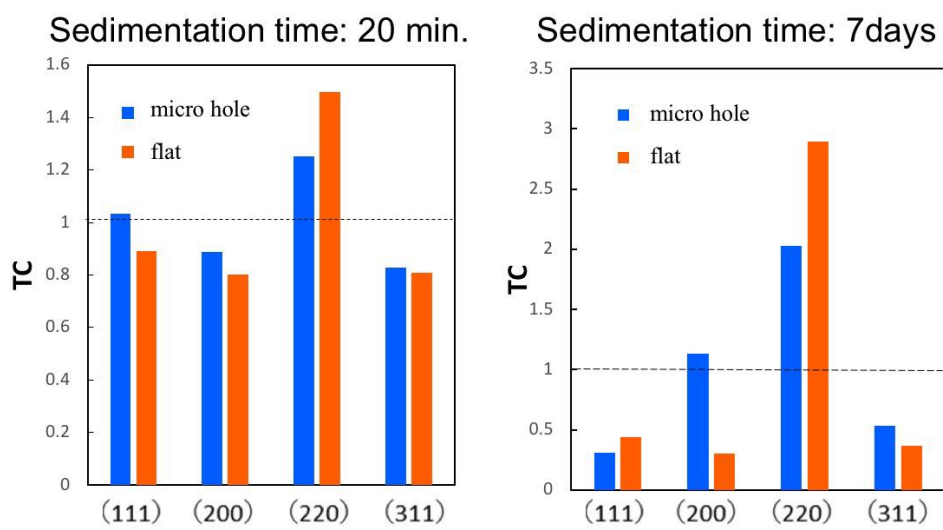


Fig. 3

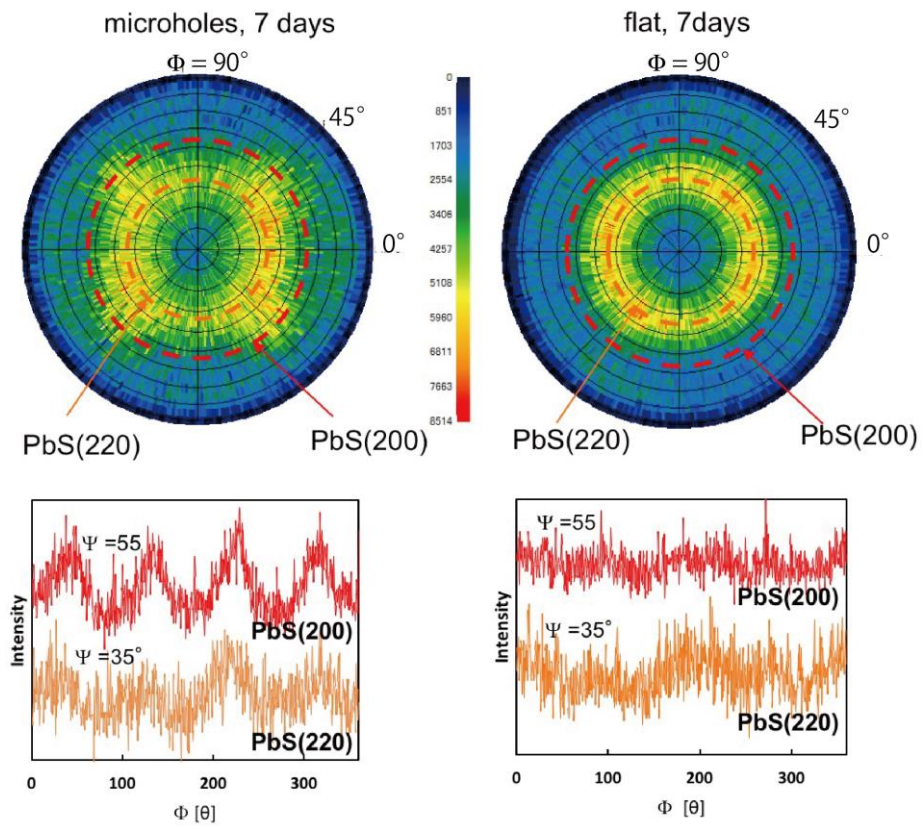


Fig. 4

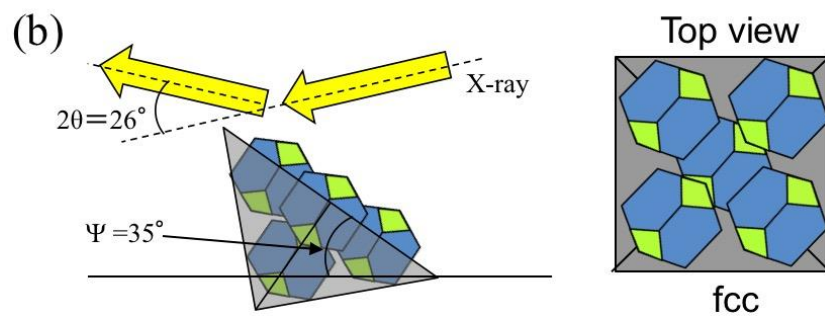
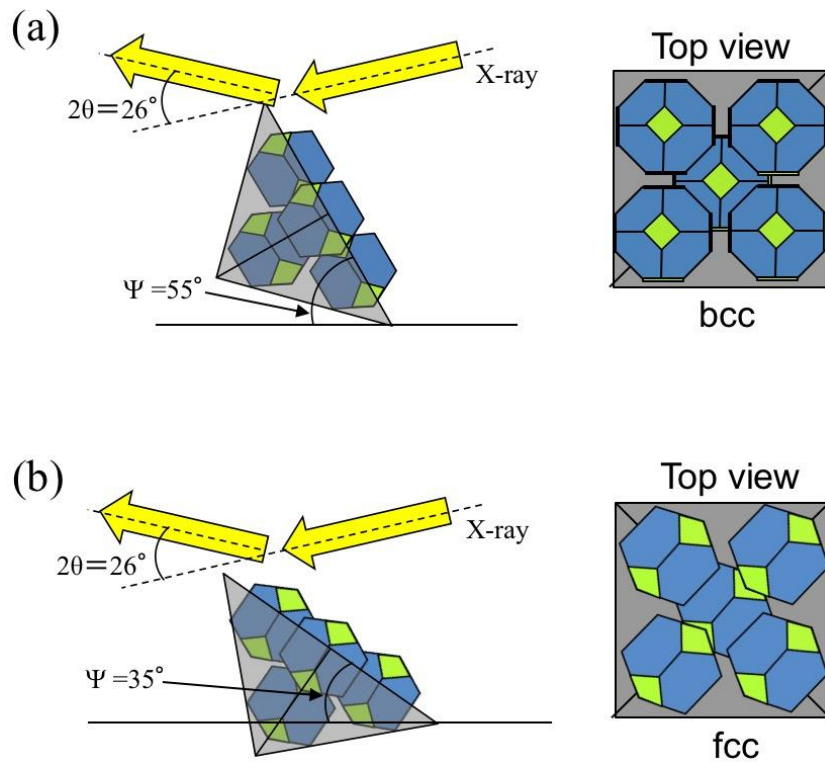


Fig.5